Thermochimica Acta, 151 (1989) 333–344
Elsevier Science Publishers B.V., Amsterdam — Printed in The Netherlands

A CALORIMETRIC DEVICE FOR THE INVESTIGATION OF TRANSFORMATIONS IN SOLIDS IN THE TEMPERATURE RANGE 100 K - 500 K

J.SCHMIDT
Institut für Werkstoffe, Technische Universität Braunschweig
West-Germany

ABSTRACT

This paper introduces a calorimetric device that can be used to observe reactions in the temperature range 100 K - 500 K. The principal part of the apparatus is an improved version of a commercial differential heat flux calorimeter. Cooling is effected by a low-temperature cryostat for liquid nitrogen into which the calorimeter is fitted. It can be heated up linearly with time at different rates using a controllable heater. These properties qualify it as a member of the class of Differential-Temperature-Scanning-Calorimeters (DTSC). The calorimeter has hitherto been applied to the investigation of the annealing effects in high-purity aluminium after low-temperature deformation /1,2/. A description shall be given here of the device and its particular characteristics. To demonstrate the efficiency of the calorimetric device reaction curves are shown which were obtained for different metals after plastic deformation at low temperatures (deformation by torsion at 77 K).

THE LOW-TEMPERATURE CALORIMETER

The low-temperature measuring device was constructed on the basis of a calorimeter "Microcalorimetre Biflux" from the firm Thermanalyse, Grenoble. Fig.1 shows the essential features of the calorimeter in its improved version. In the centre of the calorimeter two measuring cells are located. They are made of Monel tubes 0,3 mm thick and are divided by a cell-floor into cells which house the samples and reference samples (ϕ 8.8 mm x 25 mm, volume $\simeq$1.5 cm^3), and auxiliary cells for the calibration resistors (DMS 120 Ω). The calibration resistors are fixed directly underneath the cell-floor using ceramic cement. The measuring cells are connected to the heater by an upper and lower supporting flange. The heater consists of a stainless-steel ring which has six symmetrically placed holes for the insertion of heating elements; its total heating power is 250 W. The steel ring also has a hole for a Pt-100-resistor as a temperature feeler to drive a temperature control unit. The temperature controller is used to set various linear heating rates (0.5-5 K/min). A second Pt-100-resistor is fixed between the two measuring cells; it records the mean

004-6031/89/$03.50

value of the sample and reference sample temperatures. Via a linearizing element one directly obtains the voltage U(T) appropiate to the temperature T. The temperature difference ΔT between the two measuring cells is measured as the primary calorimetric signal using two thermopiles with over 200 cromel-constantan thermocouples. The voltages U(T) and $U(\Delta T)$ are recorded by a multichannel recorder as a thermogram and by a computer as a set of data.

The calibration of the calorimeter is performed by the built-in DMS-calibration resistors. Auxiliary measurements yielded the power dissipation in the supply conducting wires. This can be taken into account during calibration and an appropriate correction can be made. To be completely effective, the calorimeter must be calibrated throughout the whole measuring range for different sample masses (0g - 1.2g) and rates of heating. Fig.2 shows the calibration curve (analogue calibration factor)fitted to the various single measurements. According to this, the calorimeter has its optimum sensitivity around temperatures of 240 K.

The recorded measuring signal is not proportional to the heat flux produced by the sample reaction because of heat conducting processes. The thermopiles register the heat of reaction of the sample with a time delay. Hence the recorded measuring signal has to be corrected ("desmeared") over the intrinsic time of the calorimeter (time constant τ). The time constant is a function of the temperature, the heat capacity of the sample and measuring cell and of the pressure in the vacuumspace of the thermopiles. Fig.3 represents the time constant for a sample mass of 1.2 g as a function of the temperature. (For the method to determine the time constant see ref. /3/). It can be seen that the calibration factor and the time constant respond in opposite directions*). This control behaviour, namely high sensitivity of the device and with that a large time constant, and vice versa, is a characteristic of every heat-flux calorimeter.

In practice the calorimeter is operated at a pressure of 10^{-2} mbar in the thermopile space. As a result the time constant is larger than for higher pressures, but at the same time the calorimeter is run at the maximum possible

---

*) For the calibration factor k(T) holds /4/:

$$k(T) = \frac{1}{\alpha(T)\ R_w(T)} \qquad (1)$$

where $\alpha = U(\Delta T)/\Delta T$ is the thermopower of the thermopile material, R_w the thermal resistance of the heat conducting connectors. A large thermal resistance implies a small calibration factor, i.e. high sensitivity but at the same time a large time constant.

level of sensitivity (cf. Fig.4). The "desmearing" correction can be approximately achieved using equation (2) (see ref. /3/):

$$U_{in}^{korr}(t) = U_{out}(t) + \tau \frac{d}{dt} U_{out}(t) \qquad (2)$$

Here $U_{out}(t)$ corresponds to the recorded voltage $U(\Delta T)$ and $U_{in}^{korr}(t)$ to the corrected voltage. From $U_{in}^{korr}(t)$ one may determine the thermal power released at the sample site. Fig.5 demonstrates the quality of this simple correction for the calorimeter. The figure shows a rectangular pulse $U_{in}(t)$ applied to the measuring cell, the pulse response $U_{out}(t)$ of the calorimeter and the rectangular pulse $U_{in}^{korr}(t)$ backcalculated using equation (2). The corrections performed in this way have proved to be sufficiently accurate for the kinetic analysis of annealing reactions in deformed Cu /5/ and Al/1,2/.

To operate the calorimeter at low temperatures it is built into a low-temperature cryostat (cf. Fig.6). The cryostat produces an environment of constant low temperature for the calorimetric measuring system. The cryostat (material: stainless steel (X10CrNiTi18 9)) essentially comprises an inner vacuum space, a cooling space for liquid nitrogen (volume about 4000 cm^3) and an outer insulating vacuum space. The heat transfer from the calorimeter to the cryostat is via thin-walled stainless steel tubes and stainless steel bellows. To prevent heat conduction and convection, and uncontrollable heat transfer, the inner vacuum chamber can be evacuated. Radiation shields inside the chamber reduce to a minimum the radiation transitions. The large cooling reservoir in conjunction with a good insulating vacuum (10^{-2} mbar) constitutes a setup which is thermally stable for many hours, so that the calorimeter can even be operated at heating rates of 0.5 K/min over the whole available temperature range of 100 K - 500 K.

THE ICE-PEAK PROBLEM

It is a complicated procedure to introduce the measuring samples into the cooled calorimeter. The smallest ice crystals on the sample surface cause large endothermal noise peaks which can make the interpretation of the results of the measurement quite impossible (cf.Fig.7). This shall be demonstrated by a numerical example: Measurements on strongly cold-deformed high-purity aluminium can yield typical values of around 2 J/g /1/ for the heat of recrystallization. Since the enthalpy of fusion for ice is 333.5 J/g, we have for a typical sample mass of 600 mg, the same quantity of heat released from a 3.6 mg mass of ice! The same problem prevails on opening the calorimeter in the cold state. If not prevented, an undefinied amount of humidity immediately condenses and freezes onto the measuring cells and produces a noise peak during the measurement. To

avoid these interference effects the samples can be introduced into the measuring cell from the liquid nitrogen via a gas lock. In our case we flush continually with argon gas at slight overpressure during the process. In addition whilst the sample is actually introduced into the measuring cell, previously purified gaseous nitrogen is fed into the measuring well.

EXAMPLES OF CALORIMETRIC MEASUREMENTS ON LOW-TEMPERATURE DEFORMED METALS

Processing of the calorimeter signal (output)

After completing a measurement the recorder shows the calorimetric curve $U(\Delta T)$ and the cell temperature $U(T)$ as a function of time. Fig.8 represents a typical measurement curve for low-temperature torsion samples of high-purity aluminium Al 99.999. The calorimetric signal comprises two consecutive peaks, the signal for the cell temperature is an increasing straight line corresponding to the preset heating rate Φ. The measuring signals are processed by computer in the following steps:

(i) Construction of a baseline with the aid of a polynomial of the 2nd. to 4^{th} order.

(ii) Subtraction of the baseline and transformation of the voltages $U(\Delta T)$ into heat fluxes $\dot{E}$[mW/g] and $U(T)$ into temperatures respectively.

(iii) Separation of the two consecutive peaks into single peaks and desmearing correction using eqn.(2).

(iv) Interpolation of the supporting points (generally 250) using cubic spline functions.

(v) Integration of the peaks. Integration of the whole peak yields the energy stored in the peak E_{stor}.

For the kinetic consideration of the course of a reaction it is expedient to calculate a transformed fraction F of the reaction:

$$F(T) = \frac{1}{E_{stor}} \int_{T_o}^{T} \frac{\dot{E}(\theta)}{\Phi} d\theta \qquad (3)$$

(T_o = onset temperature of a peak)

Fig.9 shows the results after each processing stage for low-temperature torsion samples of Al99.999. With the appropiate changes in the programme, it is of course possible to kinetically analyse transformation reactions in other metallic solids, as long as a correction according to eqn.(2) can be carried out.

Results of calorimetric measurements on various low-temperature deformed metals

Plastic deformation introduces lattice defects into a metal. As a result the metal is transferred to a state of higher energy (higher free enthalpy). The lattice defects (point defects, dislocations) can, on heating to higher temperatures, anneal out depending on their activation energies. Calorimetrically one then observes the decrease in energy as an exothermal heat flux. It is from the spectrum of this heat releasing process that conclusions about the annealing mechanisms in the respective metal may be drawn.

As an example of the application possiblities of the low-temperature calorimeter, the energy-release spectra of different low-temperature deformed metals will be described. Measurements were performed on the metals Cu 99.997, Al 99.999, Ag 99.999 and Pb 99.995 after deformation by torsion in liquid nitrogen. Cu, Al and Pb were subjected to torsion up to a degree of shear strain $\gamma = 6.75$, and Ag up to $\gamma = 5.2$ (for further details see ref. /1/).

Fig.10 shows the heat flux curves of the four metals for a heating rate of $\Phi = 1.78$ K/min. After passing through the temperature interval the samples are in a recrystallized state. Each respective last peak can therefore be assigned to primary recrystallization. In Table 1 are listed some results appertaining to this peak.

The peaks at lower temperatures can be associated with the annealing of point defects (vacancies, interstitials). The annealing mechanisms occuring in the peaks are the subject of much controversial discussion to this day /6/. Comprehensive measurements on high-purity aluminium (cf. /2/ and the references to literature there in) infer that in the first peak ("low-temperature peak") those vacancies anneal out which were created during plastic deformation.

The values quoted in Table 1 only represent a small part of the information to be gained from heat flux curves. From the shift of the peaks with heating rate the curves can also be "kinetically" analysed, i.e. parameters can be determined to describe the respective reaction process (activation energy, order of reaction etc.). We shall report on this elsewhere.

TABLE 1

Results of calorimetric measurements for the recrystallization peak

metal	Cu 99.997	Al 99.999	Ag 99.999	Pb 99.995
degree of deformation γ /1	6.75	6.75	5.2	6.75
stored energy E_{stor}/Jg^{-1} $E_{stor}/Jmol^{-1}$	3.4 216	2.58 69.6	2.04 220	0.11 22.8
recrystallization temperature T_R/K	355	255	337.3	217
T_R/T_{melt}	0.26	0.27	0.27	0.36
dislocation density $N_D/cm^{-2}\cdot 10^{11+}$)	10.2	3.2	8.71	1.79

+) The dislocation density N_D, which is reduced during primary recrystallization, was estimated using the simple approximation formula $E_{stor} = N_D G b^2$ (where b = Burgers vector, G = shear modulus).

Aknowledgement

The author would like to thank Mr.H.Scholz for help in overcoming the numerous difficulties in the low-temperature calorimetric measurement technique. We are grateful to the Deutsche Forschungsgemeinschaft for financial support.

REFERENCES

/1/ F.Haeßner and J.Schmidt, Scripta Met. 22 (1988) 1917-1922.
/2/ J.Schmidt and F.Haeßner, to be published in Zeitschr.f.Physik B-Condensed Matter.
/3/ K.-H.Schönborn, Thermochimica Acta 69 (1983) 103-114.
/4/ W.Hemminger and G.Höhne, Grundlagen der Kalorimetrie, Verlag Chemie, Weinheim 1979, p.172 ff.
/5/ K.-H.Schönborn and F.Haeßner, Thermochimica Acta 86 (1985) 305-320.
/6/ H.J.Wollenberger: "Points defects" in "Physical Metallurgy", R.W.Chan and P.Haasen, eds. Elsevier Science Publishers, Amsterdam (1983) p. 1139.

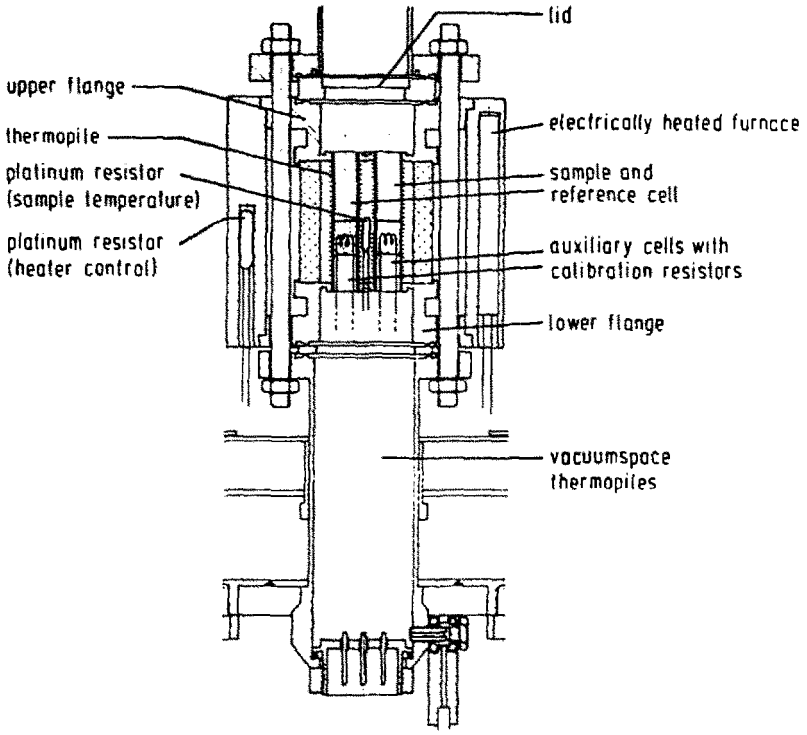

Fig.1: Cross sectional view of the calorimeter.

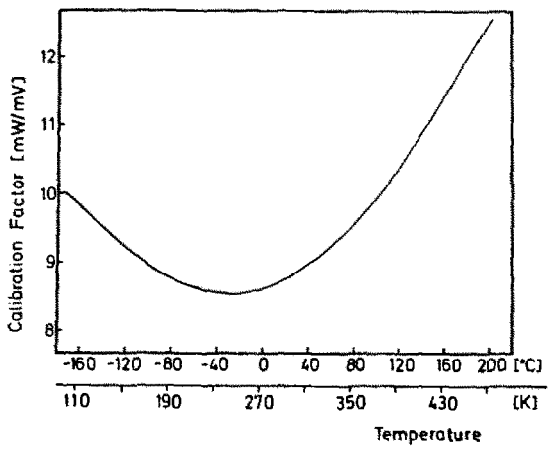

Fig.2: Calibration factor of the low-temperature calorimeter.

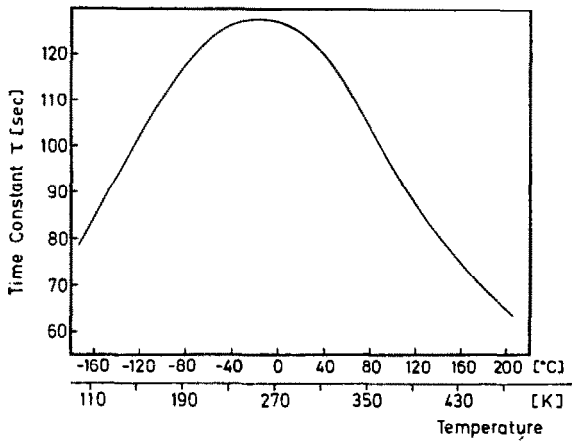

Fig.3: Time constant τ of the calorimeter (sample mass 1.2g).

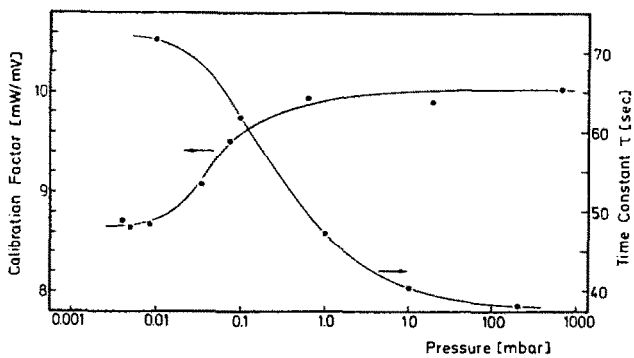

Fig.4: Influence of pressure on calibration factor and time constant in the vacuum space of the thermopiles (temperature 22°C).

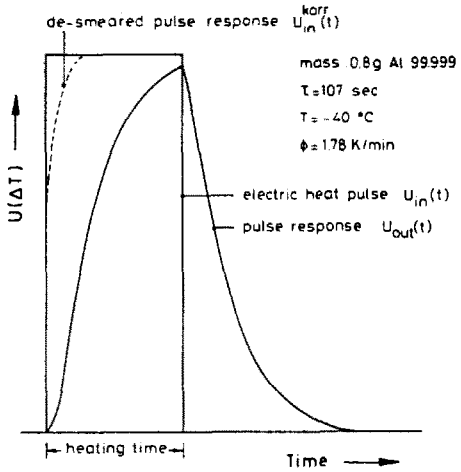

Fig.5: Example of an electric heat pulse response and the desmeared pulse response calculated from eqn.(2).

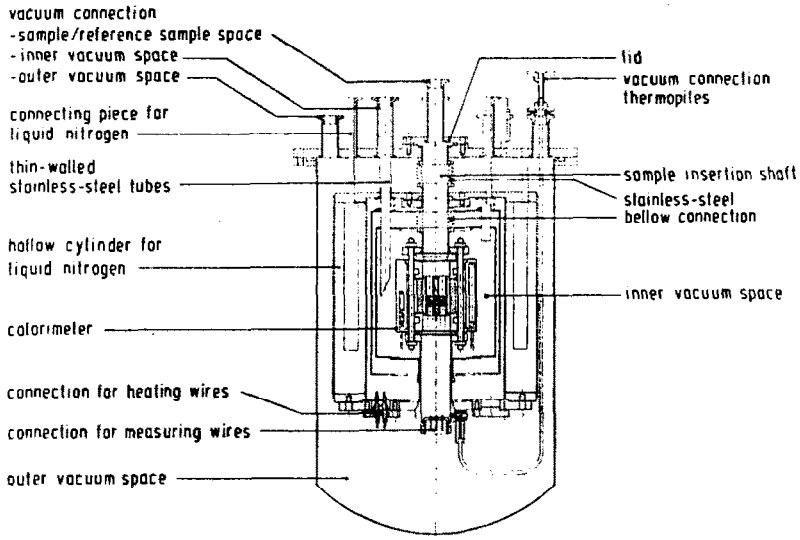

Fig.6: Cross sectional view of the low-temperature cryostat with calorimeter.

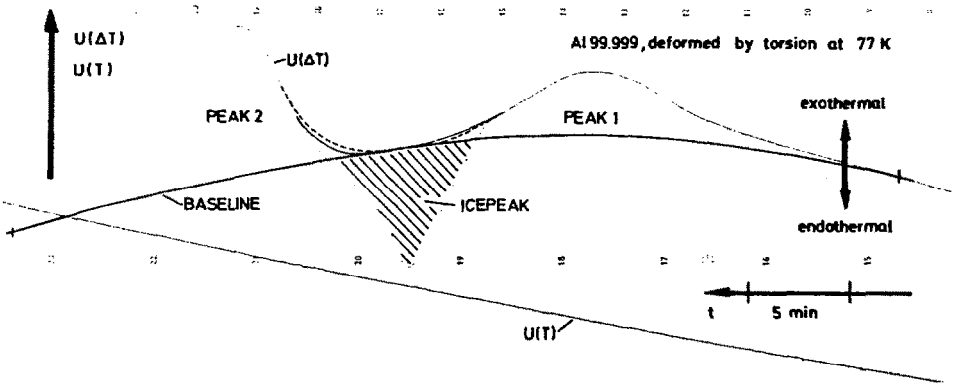

Fig.7: Anisothermal measuring curve of cold deformed aluminium. The two reaction peaks of the sample overlap with the ice-water reaction on the sample surface (for further details see text).

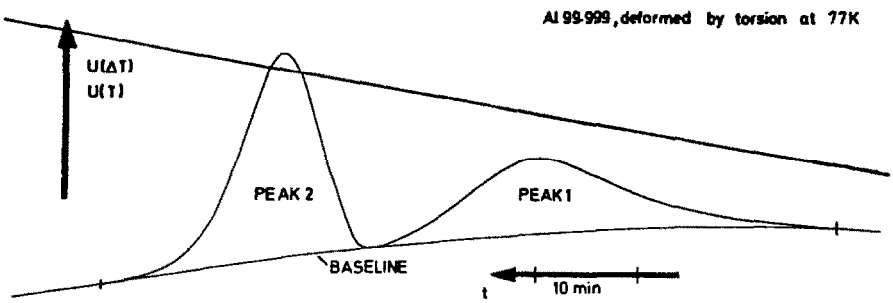

Fig.8: Typical anisothermal measuring curve with baseline and measuring signals U (ΔT) and U(T).

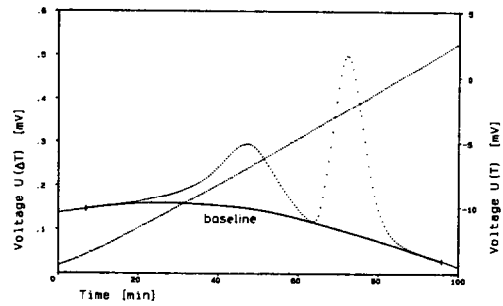

i) Construction of the baseline

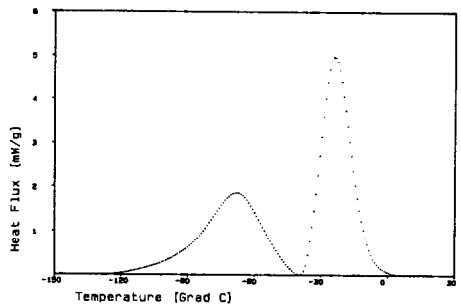

ii) Calculation of the heat flux $\dot{E}(T)$.

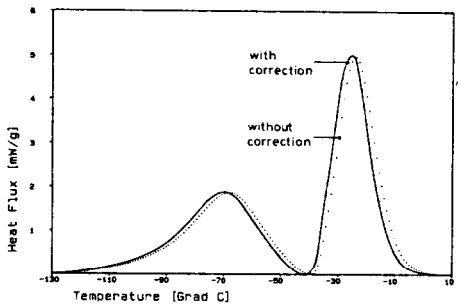

iii) Desmearing of the peaks; interpolation with cubic spline functions; determination of the peak maxima temperature.

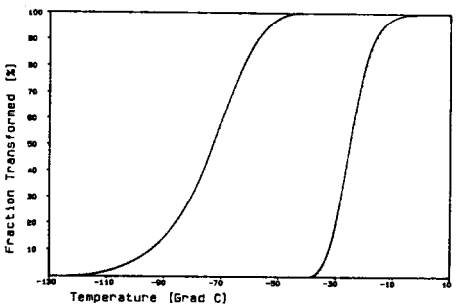

iv) Integration of the peaks: determination of the reaction energy and the fraction transformed.

Fig.9: Computer-aided evaluation of the calorimetric signals.

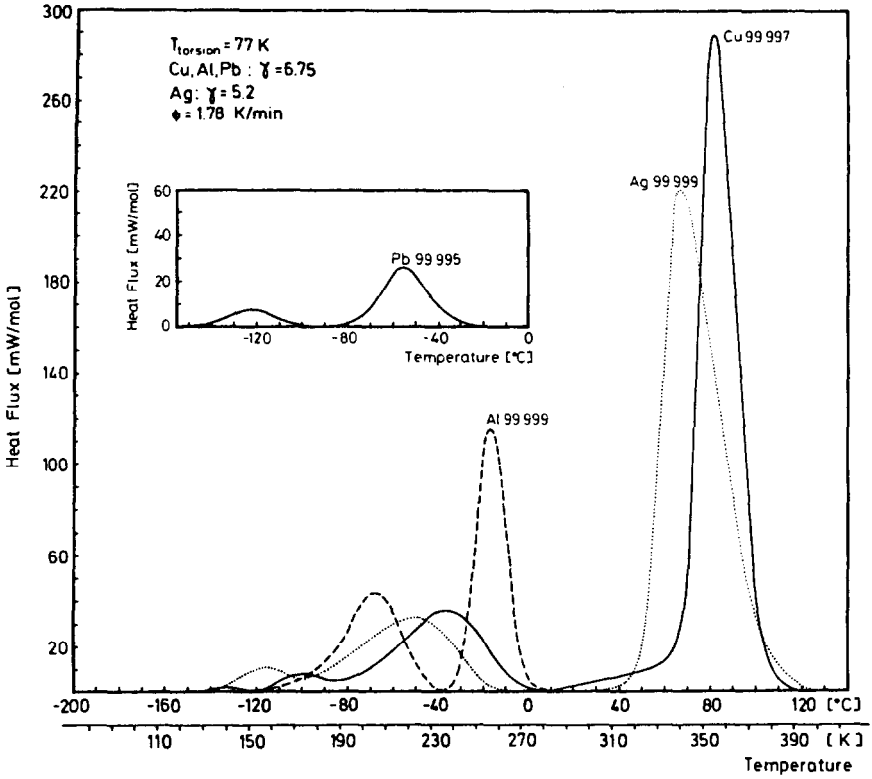

Fig.10: Heat flux curves of different metals after deformation by torsion at 77 K.